

# Одержання, структура, властивості

UDC 548.522:621.921.34-492.2

**Tao Zhang<sup>1,\*</sup>, Feng Qin<sup>1,\*\*</sup>, Lijun Zhang<sup>2,\*\*\*</sup>, Li Gao<sup>2,\*\*\*\*</sup>,  
Fanghong Sun<sup>3,\*\*\*\*\*</sup>**

<sup>1</sup>Mechanical Institute of Technology, Wuxi Institute of Technology,  
Wuxi, China

<sup>2</sup>School of Engineering Science and Technology,  
Shanghai Ocean University, Shanghai, China

<sup>3</sup>School of Mechanical Engineering, Shanghai Jiao Tong University,  
Shanghai, China

\*zhangt@wxit.edu.cn

\*\*qinf@wxit.edu.cn

\*\*\*ljzhang@shou.edu.cn

\*\*\*\*lgao@shou.edu.cn

\*\*\*\*\*sunfanghong@sjtu.edu.cn

## **HFCVD synthesis of boron-doped microcrystalline diamonds**

*Microcrystalline diamond powders are deposited directly by a HFCVD apparatus with adding amounts of trimethyl borate in gas mixture. The study establishes the relationship between the boron concentration and growth behaviors of microcrystalline diamond particles. The results present that the addition of boron and oxygen atoms increases the growth rate of diamond crystals by a factor of 1.2–1.7, moreover, does not influence the morphology and grain density of diamond particles significantly.*

**Keywords:** microcrystalline diamond particles, boron doping, growth rate, hot filament CVD.

### **INTRODUCTION**

Microcrystalline diamond powders (< 38 μm) have outstanding properties, making them suitable candidate abrasives widely employed in optical and electronic materials and components, focused on ultra-high precision finish machining processes [1, 2]. Ninety percent of the powders are fabricated from high-pressure and high-temperature (HPHT) synthesized large-sized diamonds via crushing method. As a result, they usually have imperfections both in shape and morphology [3, 4]. The literature [3] proved that regular-shaped particles with smooth surfaces behave much stronger than the needle-shaped ones and rough, blocky crystals, which as the abrasives tend to degrade the surface quality of finished workpieces and finishing efficiency.

© TAO ZHANG, FENG QIN, LIJUN ZHANG, LI GAO, FANGHONG SUN, 2019

There are recent developments in the deposition of microcrystalline diamond particles by chemical vapor deposition (CVD) methods [4–9]. Seeding and self-nucleation initiation approaches are two main current research techniques in terms of initiating diamond nucleation. Either way, CVD diamond particles generally have regular and complete crystal shapes with smooth surfaces, which stimulates interest in replacing the traditional crushing technique. However, due to particle sizes difference issue, the final crystals deposited via seeding initiation method might be not qualified for commercial powders unless postprocessed with grain-sieving. Two factors may account for the above issue, the initial seed size inhomogeneity expanding with increasing regrowth duration and the inevitable arising of spontaneous nuclei ( $< 1 \mu\text{m}$ ) developing on the substrate at the deposition, which is demonstrated in [7, 8]. Fortunately, the self-nucleation initiation approach could avoid the two issues, by which the diamond particles have not only the well-shaped morphology but a narrow range of particle sizes [6]. However, according to our knowledge, little work has been published on the deposition of isolated diamond particles with the self-nucleation initiation approach. The production of microcrystalline diamond powders via CVD method remains a challenge.

Featured with high electrical conductivity, sound chemical stability and superior mechanical properties, the diamond doped with boron attracts researchers' interests in the field of structural material [10–14]. In addition to enormous researches focus on the superconducting properties of boron-doped diamond films and large single crystals [15–17], many efforts contribute to understanding their growth behaviors and morphology. Achard [18] and Ramamurti [19] et al. demonstrated that the appropriate boron impurity could improve the crystal shapes and growth rate of single crystal diamonds. However, few attempts have been done on fabricating boron-doped microcrystalline diamond particles via CVD method and investigating the influence of boron doping on the growth characteristics of microcrystalline diamond particles. Steffen Heyer et al. successfully fabricated the boron-doped diamond nanoparticles by milling CVD diamond films [20]. Nevertheless, it was unavoidable to perform a multistep acid corrosion for purifying grain and suffer from the morphological imperfections of diamond crystals. In our previous investigation, the boron-doped diamond particles were deposited by a hot filament CVD (HFCVD) apparatus with the seeding pretreatment for the substrate. It was suggested that with 500 or 5000 ppm boron concentration, the regrowth rate of diamonds could be improved by a factor of 1–2 [8]. Unsatisfactorily, the particles have a broad range of particle sizes. Moreover, in this case, the sizes of final particles depend on that of initial seeds and are generally larger than  $2 \mu\text{m}$ .

In the present study, silicon wafers used as substrates are pretreated via scratching of very short duration for initiating the diamond nuclei with a low density. Deposition experiments are carried out using varying the boron concentration in reactive gas to have a deep insight on the effect of nucleation and growth behaviors of microcrystalline isolated diamonds. The objectives of this study are to deposit the boron-doped diamond particles with a well-defined morphology and a relatively high growth rate via HFCVD technique and meanwhile to inhibit the growth of poly-crystals.

## EXPERIMENTS DETAILS

CVD microcrystalline diamonds are produced via the HFCVD method with dynamic boron-doping [11], acetone and excessive hydrogen adopted as the reactive source, and the trimethyl borate ( $\text{C}_3\text{H}_9\text{BO}_3$ ) introduced as the source of boron.

[B]/[C] gas ratios are ranging from 0–5000 ppm. Other deposition parameters are listed in the table, which have been optimized in [6]. Mirror-polished silicon wafer with a surface area of about 100 cm<sup>2</sup> used as the substrate is fixed 10 mm below tantalum wires used as hot filaments and assembled in proper position. To reduce the agglomeration of nuclei and acquire a proper nucleation density [6, 15], uniform scratching process is applied on the substrate surfaces via commercial diamond pastes for 10–15 s. Following step is ultra-sonic bathing the substrates with deionized water and acetone.

### The deposition parameters for CVD boron-doping microcrystalline diamonds by the self-nucleation method

Parameter	Nucleation parameter	Growth parameter
The ratio of CH <sub>3</sub> COCH <sub>3</sub> to H <sub>2</sub> , %	1.5	2.0
[B]/[C] gas, ppm	0/500/5000	0/500/5000
Pressure, kPa	3.0	3.0
Bias current, A	4.0	4.0
Substrate temperature, °C	700	950
Filament temperature, °C	2000±200	2200±200
Duration, min	40	80

During the deposition process, a K-type thermocouple sensor is used to measure the temperature of the substrate as for feedback control. Field Emission Scanning Electron Microscopy (FE-SEM, Zeiss ULTRA55) is applied to characterize the morphologies and sizes of more than 500 isolated diamonds selected randomly from each substrate. Furthermore, Micro-Raman Spectroscopy (SPEX1403) is employed to examine the purity of final diamonds through detecting three randomly taken crystals from each sample.

## RESULTS AND DISCUSSION

### Influence of boron doping concentration on the nucleation characteristics of diamond particles

Figure 1 shows the morphology of diamond nuclei at different [B]/[C] gas conditions after 40 mins nucleation deposition. The nuclei exhibit a tetrahedron or cube-octahedral structure with the euhedral diamond faces clearly identifiable at all testing conditions, demonstrating that the boron-doping does not affect the morphology of isolated nucleus significantly. The size ( $Z$ ) and density ( $N$ ) of nuclei or crystals are closely associated with the inhibition of films growth and synthesis of the quantity of single microcrystalline diamonds during a vapor deposition process. The average values of  $Z$  and  $N$  in each case are measured and presented in Fig. 2. To prevent the nuclei or crystals from coalescing together,  $Z$  and  $N$  should meet the equation (1) at least [6]:

$$Z_{\max} < \sqrt{\frac{1}{\pi N}} \cdot 10^4, \mu\text{m}. \quad (1)$$

Obviously, the two factors satisfy Eq. (1) in each case. It can be found that the nuclei grow stronger exhibiting a cube-octahedral structure, and  $N$  and  $Z$  show a notable increase, as well as the increase of nuclei growth exhibits straightly climbing as the increase of boron-doping concentration. These facts explain that the

adding of trimethyl borate could accelerate the mobility of active species enhancing the nucleation rate of diamond [8]. Besides, the nucleation densities exhibit no significant difference in the lightly and heavily boron-doped conditions, specifying that the addition of boron atoms cannot increase the nucleation density on the heterogeneous substrate unlimitedly.

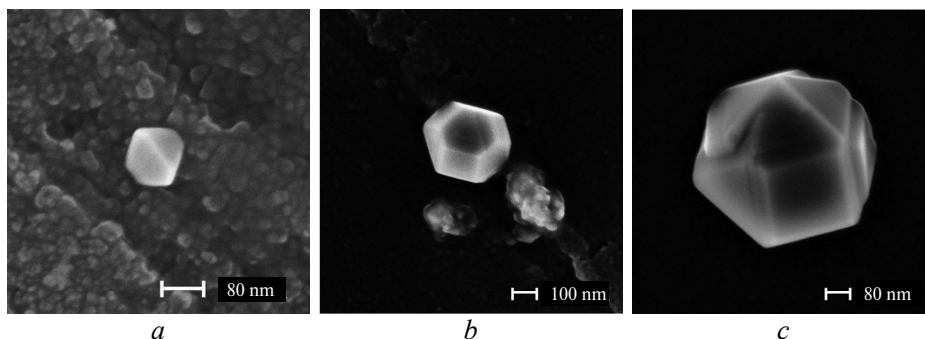


Fig. 1. The FESEM morphologies of CVD diamond nuclei grown with the different  $[B]/[C]_{\text{gas}}$ : 0 (a), 500 (b), 5000 (c) ppm.

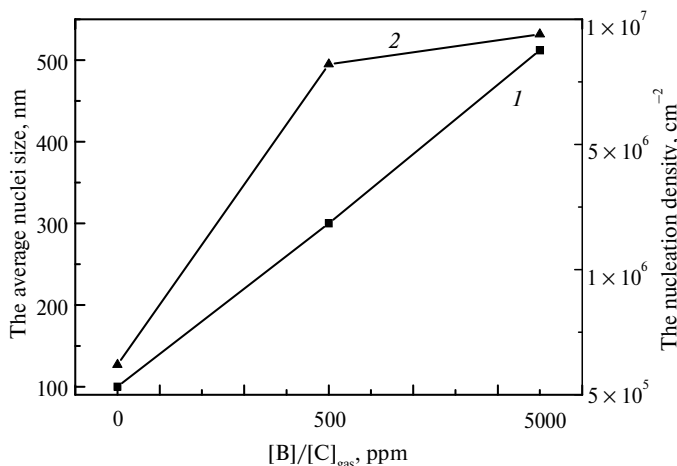


Fig. 2. The variation of average nuclei size (1) and density (2) of CVD diamond nuclei grown with the different  $[B]/[C]_{\text{gas}}$ .

### Influence of boron doping concentration on the growth characteristics of diamond particles

As shown in Fig. 3, the diamond particles with dominant  $\{111\}$  faces are obtained after 80 mins growth duration with the preexistence of isolated nuclei shown in Fig. 1. All three-species present cube octahedron and icosahedron regular shapes, which are typical morphology of single crystal diamond. The evidence points out there is no apparent link between the deposition condition of boron-doping and the morphology of final microcrystalline diamonds. However, some unwanted excrescences are appeared on the surfaces of the doped particles. Micro-Raman spectra in Fig. 4 gives that broad peaks exist at the locations of  $500$  and  $1200 \text{ cm}^{-1}$  at the boron-doping concentration of 5000 ppm, attesting the intrusion of boron atoms inside the lattices, and no clear boron peak appears at the boron-doping condition of 500 ppm, possibly due to the too small particle size and low boron concentration. The variation of average grain size ( $Z$ ) and crystal density ( $N$ )

of microcrystalline diamonds grown with the different  $[B]/[C]_{\text{gas}}$  shown in Fig. 5.  $N$  and  $Z$  satisfy Eq. (1) obviously, meeting the minimum requirement to inhibit the poly-crystals growth. Noted that, the densities of initial nuclei deposited at the intrinsic and boron-doping conditions show the obvious difference (no doping sample:  $N = 5.6 \cdot 10^5 \text{ cm}^{-2}$ ; doping samples:  $N = 1.1 \cdot 10^6 - 1.2 \cdot 10^6 \text{ cm}^{-2}$ ). However, after the growth process, there are no substantial difference on the densities of final particles produced by intrinsic and boron-doping conditions, which stabilize at  $2.0 \cdot 10^6 \text{ cm}^{-2}$ . This suggests that the nucleation density on the substrate shows some saturation, whose value depends on the pretreatment of the substrate, i.e. the grinding time of abrasives to the substrate, which has also been proved and confirmed in [6]. Furthermore, the growth rate of boron-doped isolated particles is found to be superior over that of intrinsic ones and improves remarkably with increasing the concentration of boron-doped.

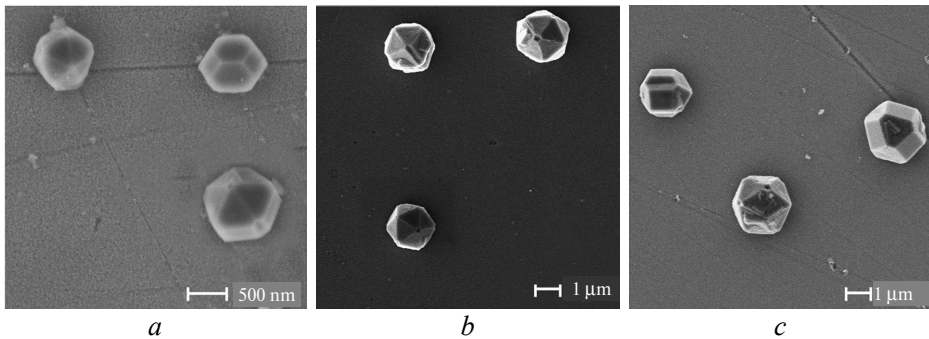


Fig. 3. The FESEM morphologies of CVD microcrystalline diamonds grown with the different  $[B]/[C]_{\text{gas}}$ : 0 (a), 500 (b), 5000 (c) ppm.

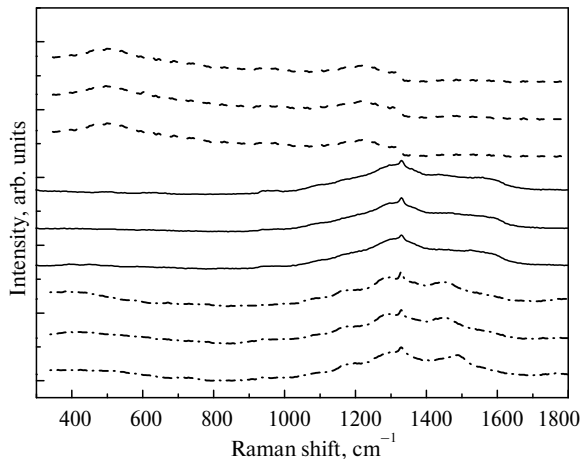


Fig. 4. Micro-Raman spectra of CVD microcrystalline diamonds grown with the different  $[B]/[C]_{\text{gas}}$ : 0 (· · · ·), 500 (—), 5000 (---) ppm.

The introduction of the trimethyl borate ( $\text{C}_3\text{H}_9\text{BO}_3$ ) could directly improve the growth rate of single grain, and three factors may contribute to the improvement. Firstly, the trimethyl borate undergoes thermal decomposition, then breaks its carbon oxygen bond to generate methyl radical and borylate group with hanging bonds. The methyl radical can participate diamond deposition while the borylate group may not be decomposed fully due to its atomic vacancy but directly connect

the atomic vacancy of the diamond. As the group volume of the borylate group exceedingly greater than that of the methyl radical, its participation can significantly improve the growth rate of diamond. Secondly, the borylate group enters diamond lattice during the reaction and causes the lattice distortion or even produces screw dislocations as a result of the different atomic radii of boron and carbon. The lattice distortions reduce the interface energy of the system, thereby speeding the reacting rate of the active species. Besides, due to the imperfections of crystals, unwanted excrescences could be detected on the surfaces of boron-doped diamonds. Thirdly, dehydrogenating rate at the diamond surface is also an important factor affecting diamond growth rate. During the intrinsic growth, the hydrogen debonding off diamond surface mainly depends on the integration of hydrogen atoms from the reactive species (104.2 kcal/mol H–H binding energy) while after doping the oxygen-free radical (–OH) from the trimethyl borate decomposition can also abstract the hydrogen at the diamond surface with even higher binding energy of 119 kcal/mol, which causes easier peel-off for surface hydrogen atoms to provide vacancies for diamond growth and speed its growth rate [21]. The similar conclusion can be inferred from Ref. [8].

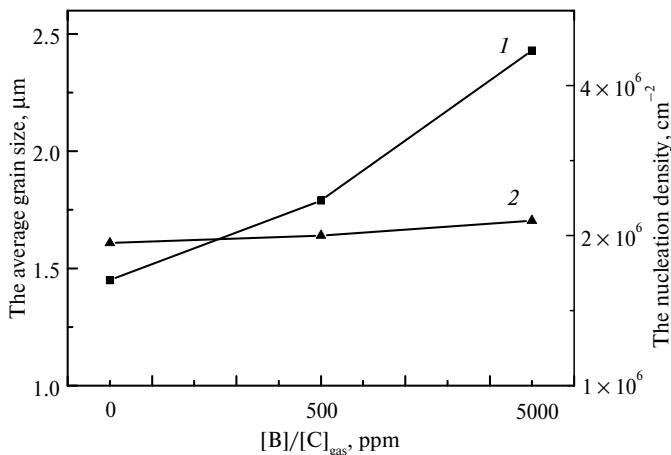


Fig. 5. The variation of average grain size (1) and crystal density (2) of CVD microcrystalline diamonds grown with the different  $[B]/[C]_{\text{gas}}$ .

Additionally, the boron-doping diamond particles with various average grain sizes can be obtained by adjusting the deposition time. Figure 6 presents the FE-SEM morphologies of boron-doped isolated diamonds with the  $[B]/[C]_{\text{gas}}$  ratio of 5000 ppm under the deposition time of 100 min, whose average grain size is about 2.1  $\mu\text{m}$ . The most particles are the nearly ball-shape, whose mechanical properties are substantially higher than ones with the needle shape produced from the crushing approach [22]. What's more, these particles have an extremely narrow size range, meeting the size and size distribution requirements of the type of M1/2 of commercial powders without sieving grain.

## CONCLUSIONS

The HFCVD has been performed to deposit the microcrystalline diamond powders with the cubic-crystal shapes via the self-nucleation initiation and doping trimethyl borate method. The  $[B]/[C]_{\text{gas}}$  atomic ratio is fixed at 0, 500, and 5000 ppm to research the effect of boron impurities on the growth characteristics of microcrystalline diamond particles. It is found that the boron-doping technique

does not influence the morphology and grain density of diamond particles significantly. The most particles show a cube octahedron or icosahedron structure, and they are isolated. Moreover, the introduction of boron and oxygen atoms has improved the growth rate of diamond particles for 1.2–1.7 times.

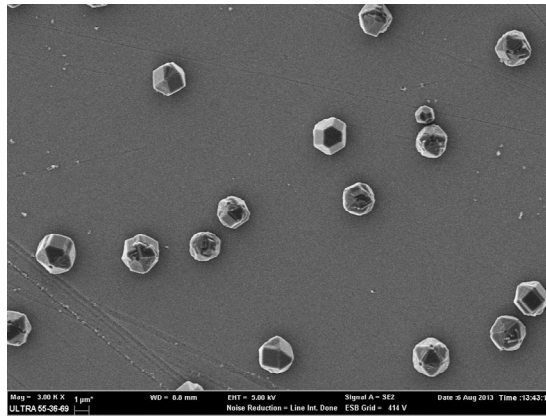


Fig. 6. The FESEM morphologies of CVD boron-doping diamond powders grown by the self-nucleation initiation method.

## FUNDING

This research is supported by the National Natural Science Foundation of China (No. 51605280) and Scientific and Technological Innovation Team Foundation of Wuxi Institute of Technology.

*Мікрокристалічні порошки алмазу осаджуються безпосередньо з допомогою апарата HFCVD з додаванням деякої кількості триметилбората в газову суміш. Дослідження встановлює зв'язок між концентрацією бору та характеристиками росту мікрокристалічних алмазних частинок. Результати показали, що додавання атомів бору та кисню збільшує швидкість росту кристалів алмазу в 1,2–1,7 рази, крім того, не впливає суттєво на морфологію та щільність зерен алмазних частинок.*

**Ключові слова:** мікрокристалічні алмазні частинки, легування бором, швидкість росту, гарячі нитки CVD.

*Мікрокристаллические алмазные порошки наносятся непосредственно с помощью устройства HFCVD с добавлением некоторого количества триметилбората в газовую смесь. Исследование устанавливает связь между концентрацией бора и характеристиками роста микрокристаллических алмазных частиц. Результаты показали, что добавление атомов бора и кислорода увеличивает скорость роста кристаллов алмаза в 1,2–1,7 раза, кроме того, не оказывает существенного влияния на морфологию и плотность зерен частиц алмаза.*

**Ключевые слова:** микрокристаллические алмазные частицы, легирование бором, скорость роста, горячая нити CVD.

1. May P.W. CVD diamond: a new technology for the future? *Endeavour*. 1995. Vol. 19, no. 3. P. 101–106.
2. Filatov Y.D., Vetrov A.G., Sidorko V.I., Filatov A.Y., Kovalev S.V. A mechanism of diamond-abrasive finishing of monocrystalline silicon carbide. *J. Superhard Mater.* 2013. Vol. 35, no. 5. P. 303–308.
3. Sung C. M. Brazed diamond grid: a revolutionary design for diamond saws. *Diamond Relat. Mater.* 1999. Vol. 8, no. 8–9. P. 1540–1543.
4. Schwarz S., Rottmair C., Hirmke J., Rosiwal S., Singer R.F. CVD-diamond single-crystal growth. *J. Cryst. Growth*. 2004. Vol. 271, no. 3–4. P. 425–434.

5. Achard J., Tallaire A., Sussmann R., F. Silva F., Gicquel A. The control of growth parameters in the synthesis of high-quality single crystalline diamond by CVD. *J. Cryst. Growth*. 2005. Vol. 284, no. 3–4. P. 396–405.
6. Zhang T., Liu X., Sun F., Zhang Z. The deposition parameters in the synthesis of CVD microcrystalline diamond powders optimized by the orthogonal experiment. *J. Cryst. Growth*. 2015. Vol. 426. P. 15–24.
7. Zhang T., Wang X., Shen B., Sun F., Zhang Z. The effect of deposition parameters on the morphology of micron diamond powders synthesized by HFCVD method. *J. Cryst. Growth*. 2013. Vol. 372. P. 49–56.
8. Zhang T., Wang L., Sun F., Shen B., Zhang Z. The effect of boron doping on the morphology and growth rate of micron diamond powders synthesized by HFCVD method. *Diamond Relat. Mater.* 2013. Vol. 40. P. 82–88.
9. Chung H.-K., Sung J.C. The CVD growth of microcrystals of diamond. *Diamond Relat. Mater.* 2001. Vol. 10, no. 9–10. P. 1584–1587.
10. Sidorov V.A., Ekimov E.A. Superconductivity in diamond. *Diamond Relat. Mater.* 2010. Vol. 19, no. 5–6. P. 351–357.
11. Wang L., Lei X., Shen B., Sun F., Zhang Z. Tribological properties and cutting performance of boron and silicon doped diamond films on Co-cemented tungsten carbide inserts. *Diamond Relat. Mater.* 2013. Vol. 33. P. 54–62.
12. Chepugov A., Ivakhnenko S., Garashchenko V. The study of large semiconducting boron doped single crystal diamond sectorial structure. *Physica Status Solidi (c)*. 2014. Vol. 11, no. 9–10. P. 1431–1434.
13. Nantaphol S., Channon R. B., Kondo T., Siangproh W., Chailapakul O., Henry C.S. Boron doped diamond paste electrodes for microfluidic paper-based analytical devices. *Analytical Chemistry*. 2017. Vol. 89, no. 7. P. 4100–4107.
14. Tarelkin S., Bormashov V., Kuznetsov M., Buga S., Terentiev S., Prikhodko D., Golovanov A., Blank V. Heat capacity of bulk boron-doped single-crystal HPHT diamonds in the temperature range from 2 to 400 K. *J. Superhard Mater.* 2016. Vol. 38, no. 6. P. 412–416.
15. Iniesta J., Michaud P. A., Panizza M., Cerisola G., Aldaz A., Comminellis C. Electrochemical oxidation of phenol at boron-doped diamond electrode. *Electrochim. Acta*. 2001. Vol. 46, no. 23. P. 3573–3578.
16. Kamo M., Sato Y., Matsumoto S., Setaka N. Diamond synthesis from gas phase in microwave plasma. *J. Cryst. Growth*. 1983. Vol. 62, no. 3. P. 642–644.
17. Kumar D., Chandran M., Rao M.S.R. Effect of boron doping on first-order Raman scattering in superconducting boron doped diamond films. *Appl. Phys. Lett.* 2017. Vol. 110, no. 19. P. 191602.
18. Achard J., Silva F., Issaoui R., Brinza O., Tallaire A., Schneider H., Isoird K., Ding H., Kon S., Pinault M.A., Jomard F., Gicquela A. Thick boron doped diamond single crystals for high power electronics. *Diamond Relat. Mater.* 2011. Vol. 20, no. 2. P. 145–152.
19. Ramamurti R., Becker M., Schuelke T., Grotjohn T. A., Reinhard D.K., Asmussen J. Deposition of thick boron-doped homoepitaxial single crystal diamond by microwave plasma chemical vapor deposition. *Diamond Relat. Mater.* 2009. Vol. 18, no. 5–8. P. 704–706.
20. Heyer S., Janssen W., Turner S., Lu Y.G., Yeap W.S., Verbeeck J., Ken H., Krueger A. Toward deep blue nano hope diamonds: heavily boron-doped diamond nanoparticles. *ACS nano*. 2014. Vol. 8. P. 5757–5764.
21. Su Y., Li H.D., Cheng S.H., Zhang Q., Wang Q. L., Lv X.Y., Zou G.T., Pei X.Q., Xie J.G. Effect of N<sub>2</sub>O on high-rate homoepitaxial growth of CVD single crystal diamonds. *J. Cryst. Growth*. 2012. Vol. 351, no. 1. P. 51–55.
22. Skury A.L.D., Bobrovnichii G.S., Monteiro S.N. A parametric relationship for synthesized diamond powder. *Diamond Relat. Mater.* 2006. Vol. 15, no. 1. P. 61–66.

Received 02.01.18

Revised 02.01.18

Accepted 04.04.18